NBSIR 82-2473

Entrainment and Heat Flux of Buoyant Diffusion Flames

U.S. DEPARTMENT OF COMMERCE
National Bureau of Standards
Washington, DC 20234

February 1982

Final Report

U.S. DEPARTMENT OF COMMERCE
NATIONAL BUREAU OF STANDARDS

NBSIR 82-2473

ENTRAINMENT AND HEAT FLUX OF BUOYANT DIFFUSION FLAMES

B. J. McCaffrey and G. Cox

U.S. DEPARTMENT OF COMMERCE
National Bureau of Standards
Washington, DC 20234

February 1982

Final Report

U.S. DEPARTMENT OF COMMERCE, Malcolm Baldrige, *Secretary*
NATIONAL BUREAU OF STANDARDS, Ernest Ambler, *Director*

TABLE OF CONTENTS

LIST OF FIGURES

LIST OF TABLES

NOMENCLATURE

A	centerline velocity correlation parameter (Table I)
B	centerline temperature rise correlation parameter (Table I)
C_p	specific heat of gases
e	combustion efficiency
F_o	source buoyancy parameter defined after eq. (10)
g	gravitational constant
H(z)	convective heat flux defined by eq. (2)
L	flame length, $z' = 0.2\ \text{m kW}^{-2/5}$
m(z)	mass flow rate defined by eq. (1)
M	constant defined after eq. (14)
n	power of centerline V and AT correlations
Q	heat release rate of fire
T	temperature
AT	temperature rise above ambient, $T-T_o$
V	vertical gas velocity
x	radial or transverse coordinate
z	vertical or axial coordinate
z'	scaled axial coordinate = $z/Q^{2/5}$
α,β	parameters used for width of velocity profile eq. (11)
a_e	normal entrainment coefficient
Γ_λ	density deficit defined by eqs. (3) and (4)
κ_λ	parameter defined after eq. (12)
λ	ratio of widths of temperature rise and velocity profiles
ρ	gas density

σ	l/e of centerline value
χ	radiative fraction

Subscripts

m	mean temperature (appendix)
o	ambient conditions
P	plume region
RAD	radiative component
T	temperature
TOT	total or nominal
V	velocity

Superscripts

'	fluctuating component
–	time-averaged value
~	non-dimensional centerline temperature rise and velocity parameters defined by eqs. (9) and (10)

Entrainment and Heat Flux of Buoyant Diffusion Flames

B. J. McCaffrey and G. Cox*

National Bureau of Standards
Washington, D. C. 20234

Measurements of the vertical component of velocity in buoyant diffusion flames from extended sources by both cross-correlation [1][1] and pressure probe techniques [2] incorporating time-average signal processing appear to overestimate the transverse size of these systems based on a heat balance using measured mean flux. By utilizing measurements of the radiative fraction of the flames, and forcing a mean flux heat balance, estimates of the transverse variation of velocity are obtained and expressions for flame entrainment and convective heat flux are determined. The use of mean values is seen to lead to both overestimates as well as underestimates of total flux due to turbulent transport.

Key words: buoyancy; cross-correlation; diffusion flames; entrainment; heat flux; radiation; turbulence.

1. Introduction

Mathematical modeling of fire is being approached by two main techniques. Field models attempt to solve the partial differential equation describing the fluid motion throughout the flow field [3] while zone models attempt the less ambitious task of solving ordinary differential equations within identifiable flow regimes, e.g., near walls, near ceilings, within the plume, etc. [4, 5].

---

* Fire Research Station, Borehamwood, England.

[1] Numbers in brackets indicate the literature references at the end of the paper.

The zonal approach is closer to immediate application but field models should, in the long term give more general and detailed predictions. It is now possible with zone models to make predictions of the outcome of a fire in a single compartment given information about the geometry of the room, properties of the wall material, the nature and size of the ignition source, the fuel array and its burning characteristics, etc. References [4] and [5] give examples of the kinds of input required and an assessment of how well these models reproduce reality. One of the aims of this effort was to make these models modular in form such that each portion which describes a distinct physical phenomenon, e.g., flame radiation or turbulence characteristics, could easily be replaced as new information becomes known. The models could then incorporate the best physics and chemistry available at the time.

One of the portions or submodels of these computer codes involves the entrainment of air into the fire plume. Fresh air enters the lower portion of the enclosure opening, is sucked or entrained into the fire, becomes vitiated as the combustion process takes place, and is delivered to the upper portion of the room above the thermal discontinuity (horizontal layer separating the cool fresh air from the hot combustion products). From there the products flow out the top portion of the door. The fire is thus thought of as a pump. Its characterization is coupled to the hydrostatic equations describing the flow through the opening via the height of the thermal discontinuity.

To describe fire correctly an accurate knowledge of the air and gas flow through the enclosure is critical. The hydrostatic model for doorway flow has already been demonstrated to be quite adequate [6]. The fire entrainment portion however appears to be conceptually weak since it involves, for the most part, formulations based on point source plume theory which should not be expected to hold in the accelerating region near the base of the flames.

The present work is an attempt to fill this void. A valid phenomenological expression was sought for the entrained mass flow rate as a function of the fire size and the height above the burning surface. This was accomplished using the results of two separate measurement techniques. Differences found in the two measurements were reconciled by the use of an additional independent observation, namely, a measure of the radiative fraction of these flames. The results are applicable to a fire in the open, which is one that is not impeded or otherwise influenced by any effects due to the presence of an enclosure. The effects of the enclosure on these results must still be considered.

2. Analysis

Assuming cyclindrical symmetry with axial coordinate z and radial coordinate x the stationary value of the mass flow rate, m(z), and convected energy flux, H(z) at any height z are

$$m(z) = \int_0^\infty \overline{\rho v}\ 2\pi x dx \tag{1}$$

$$H(z) = \int_0^\infty \overline{\rho v \Delta T}\ C_p\ 2\pi x dx \tag{2}$$

where ρ, v and ΔT are the time varying density, vertical velocity and temperature rise above ambient. It is usual now to assume that

(i) $\overline{\rho v} = \bar{\rho} \cdot \bar{v}$ and $\overline{\rho v \Delta T} = \bar{\rho} \cdot \bar{v} \cdot \overline{\Delta T}$

(See the Appendix for a discussion of the effect of neglecting turbulent transport. Above the flame region ($\Delta T \to 0$) neglect of turbulence will lead to underestimates of the flux while in the flame the errors appear to be in the opposite direction.)

(ii) The gas is ideal with no composition changes

$$\rho_o T_o = \rho(T_o + \Delta T)$$

(iii) The transverse velocity and temperature rise profiles may be represented by Gaussian distributions

$$\bar{v} = V(z)\ \exp\left[-\left(\frac{x}{\sigma_v}\right)^2\right]; \quad \overline{\Delta T} = \Delta T(z)\ \exp\left[-\left(\frac{x}{\sigma_T}\right)^2\right]$$

where σ is the radial distance at which the variable falls to l/e of its centerline value. Defining $\lambda = \sigma_T/\sigma_v$, substitution in (1) and (2) yields

$$m(z) = \rho_o \pi \sigma_v^2 V(z) \int_o^1 \frac{dy}{\frac{\Delta T(z)}{T_o}\ y^{1/\lambda^2} + 1} \tag{3}$$

where $y = \exp\left[-\left(\frac{x}{\sigma_v}\right)^2\right]$ and the subscript o denotes ambient conditions. Then

$$m(z) = \pi \sigma_v^2 V(z)\ \rho_o\ \Gamma_\lambda\ (\Delta T/T_o) \tag{4}$$

and

$$H(z) = \pi \sigma_v^2 V(z) C_p T_o \rho_o \left[1 - \Gamma_\lambda (\Delta T/T_o)\right] \tag{5}$$

where C_p has been assumed constant. Comparing with eq. (4) for the total mass

$$H(z) = m(z) C_p T_o \left[\frac{1}{\Gamma_\lambda (\Delta T/T_o)} - 1\right] \tag{6}$$

where $\Gamma_\lambda(\Delta T/T_o)$, a function of the centerline temperature rise, depends only upon the transverse variation of temperature, σ_T.

Equation *(4)* states that the mass flow rate is equal to the ambient density times the centerline velocity times a representative area, $\pi\sigma_v^2$, modified by $\Gamma_\lambda (\leq 1)$ which accounts for density decrease due to the fact that the gases are hotter than the ambient.

For various values of λ eq. *(3)* can be integrated analytically. Figure 1 shows the variation of Γ_λ with centerline temperature rise for a variety of assumed σ_T or λ. The limits are $\Gamma = 1$ for $\sigma_T = 0$, that is, the gases are at ambient temperature. For $\sigma_T \to \infty$, the temperature profile is completely horizontal or independent of x and equal to the centerline value. Neither of these two limits is appropriate for a flame. Experiments indicate that λ is of order 1, i.e., the temperature rise profile is of similar width to the velocity profile. For buoyant flames the cross-hatched area shows the range of experimentally determined λ [1, 2]. Note these have $\lambda < 1$ i.e., the velocity profile is wider than the temperature rise profile, a result contrary to the classical plume experimental findings of $\lambda = 1.16$ [7]. At large z, high above the flame tip where $\Delta T \to 0$, Γ_λ converges to 1 since most of the gas consists of entrained ambient air. Near the burner $\Delta T/T_o$ can be as high as 3 or 4 leading to Γ_λ of the order 0.5. This would produce large errors if the ambient density were used throughout.

2.1 Data

The quantities in the right hand side of eq. *(4)* have recently been measured by two independent techniques: Cross correlation of naturally occurring thermal and ionization fluctuations [1], and an impact pressure probe/sensitive manometer combined with a thermocouple for density determination [2]. The same porous refractory gas burner (0.3 m square) chosen to simulate the unwanted fire (a very buoyant diffusion flame emanating from an area source) was used by both investigators. Natural gas was employed as the fuel and the flow of gas corresponded to the mass burning rates of realistic materials (150 to 600 kW/m^2). For these buoyancy dominated systems it is the large scale fluctuating (in time and space) nature of these flames that makes measurement very difficult. The complete details of the two experimental techniques are contained in references [1] and [2].

Based on time-averaged centerline values of V and AT the flame can be considered to be divided into three distinct regimes: (1) A continuous flame region, starting from the surface of the burner with V close to zero at the surface and rising with the height above the burner, z, to the 1/2 power. AT is approximately constant over this regime. Higher up is (2), an intermittent regime, with pulsating flame (— 3Hz) exhibiting approximately constant V and AT falling with z to the first power. Still higher is (3) the plume region which is, most of the time, free of flames with $V \sim z^{-1/3}$ and AT $\sim z^{-5/3}$ as predicted by conventional plume theory. Throughout the three regimes and indistinguishable among these is the consistency of the buoyancy relation, $V/\sqrt{2gz\Delta T/T_o}$ which has a value of approximately 0.9. This states that throughout these flame systems velocities are derivable from static pressure differences due solely to buoyancy created from temperature differences generated from the heat release of the combustion process.

During these studies the scaling for Q, the nominal heat release rate or net calorific potential has been determined experimentally as have the three regime demarcations. The scaling reduces all the data from different size fires to a single universal curve. The length scale is $z/Q^{2/5}$, the velocity scale is $V/Q^{1/5}$, and the temperature requires only reference to ambient, AT = $T - T_o$. The flame regime is thus independent of Q. The flame - intermittent intersection is at a scaled height of 0.08 $m \cdot kW^{-2/5}$ and the intermittent - plume intersection at 0.20 $m \cdot kW^{-2/5}$. From reference [2] the visible flame height is seen to correspond to the top of the intermittent regime, which was determined by a change in the character of both the velocity and temperature rise measurements. At scaled z higher than this value, the centerline velocity and temperature rise begin to fall as dictated by point source plume theory. The combustion zone is thus over at $z/Q^{2/5}$ corresponding to the intermittent - plume intersection or visible flame height.

Table I contains the experimental centerline and radial flame parameters required by eq. (4) as determined by the two techniques.

It is quite evident from table I that problems of comparison or significant differences are going to lie in the transverse or radial measurement. Axial velocities are within 4% of each other and temperature rise measurements fall within 10%. Note that 10% is not a critical amount since centerline temperature enters eq. (4) only through Γ_λ. For present purposes the centerline measurements are virtually the same. However, significant differences do exist in the radial measurement and the mass flow rate is a function of σ_v to the second power thus amplifying differences in that measurement. Note that σ_v and λ in the table are a least-squares fit of considerably scattered data. It is difficult and may be purely speculative to try to accurately assess the experimental errors in the two techniques for those radial measurements. Near the centerline velocities have a somewhat preferred direction. However, as one moves away from the centerline, in the "wings," vertical components of velocity are approaching zero, and temperatures are approaching ambient. Horizontal components of velocity are the same order of magnitude as the vertical components due to mixing resulting from the large scale, coherent eddy motion characteristic of these systems. Any inaccuracies due to inherent wavering or meandering of the fire would also be present in both measurements.

The most likely experimental error common to both techniques results from the assumption that the velocity measured is only that of the vertical component. In flows with strong recirculation the yaw insensitivity of the pressure probe and the possibility of broad fronts of information highly correlated at right angles to their direction of

Table I. Comparison of Fire Properties Determined from Two Techniques

Q: 15-60 kW

	Axial						Transverse	
	$V/Q^{1/5} = A(z/Q^{2/5})^n$; $\Delta T = B(z/Q^{2/5})^{2n-1}$							
	CONTINUOUS FLAME		INTERMITTENT		PLUME			
	$z/Q^{2/5} < 0.08$, $n = 1/2$		$0.08 < z/Q^{2/5} < 0.2$, $n = 0$		$z/Q^{2/5} > 0.2$, $n = -1/3$			
	A	B	A	B	A	B	σ_V	λ
CROSS - CORRELATION (Cox and Chitty, 1980)	6.83	880	1.85	70	1.08	23.6	$0.14z + 0.023\, Q^{2/5}$	1/1.4
IMPACT PROBE (McCaffrey, 1979)	6.84	800	1.93	63	1.12	21.6	$0.46 \frac{z}{Q^{2/5}} + 0.013\, Q^{1/2}$ $(0.12z + 0.019\, Q^{2/5})$	1/1.2

UNITS: $z, \sigma_\omega, \sigma_T$ [m]; V [m/s]; Q [kW]; ΔT [°C, K] flow, i.e., flame fronts, passing the sensors at an oblique angle to the vertical would produce overestimates of velocity. This effect is likely to be greatest in the wings. It is clear that although the two techniques differ in their measurements of plume spread they both tend to give an overestimate of total heat flux based on mean flux balance. Terai and Nitta also reported similar difficulties [8]. What is needed is an additional method of obtaining the radial information which would complement the above results and not be subject to the same inaccuracies of those measurements. One such idea involves the convective heat flux of the fire and utilizes an additional measurement of the total radiative power output of the fire.

2.2 Radiative Power Output

Assuming complete combustion, the value of the convective heat flux at the intermittent-plume intersection will be equal to the energy supplied to the burner, Q, minus what is radiated away over the combustion region from the base of the burner up to the visible flame tip or intermittent-plume intersection. If this radiative fraction is known from an additional independent measurement, then eq. (5) can be solved explicitly for σ_v.

Let us define χ, the radiative fraction, as the total radiative power output of the fire divided by the total heat release rate, Q. ($Q = H + Q_{radiative}$)

$$\frac{H}{\hat{Q}} = 1 - \chi \tag{7}$$

Substituting this expression into eq. (5) and evaluating all the quantities in the plume region yields the radial width at the flame tip:

$$\sigma_v = \left\{ \pi C_p T_o \rho_o A_p \; z'^{-1/3} \left[1 - \Gamma_\lambda \left(\frac{B_p}{T_o} \; z'^{-5/3} \right) \right] \right\}^{-1/2} .$$

$$(1 - \chi)^{1/2}\ Q^{2/5} \tag{8}$$

all evaluated at $z' = z/Q^{2/5} = 0.2\ \mathrm{m \cdot kW^{-2/5}}$ from table I and figure 1.

It is interesting to note that for χ independent of Q, the proper transverse scale is $Q^{2/5}$ which is the same as that determined for the longitudinal scale [2]. Markstein [9] in fact has demonstrated the consistency of χ over an extremely wide range of Q for propane. Unfortunately these results were for very large velocity flames issuing from small nozzles. For the moderate-sized or developing fire buoyancy is dominating, the processes are not well understood, and the burning rate per unit area and χ turn out to be increasing functions of source area for a given fuel [10]. Similarly for a fixed source area different materials will exhibit different radiative characteristics resulting in different burning rates per unit area and different χ. The effect of fuel in this case was simulated by varying gas flow rates, Q, to the burner.

The radiative fraction of the present flame system has been recently measured in a manner similar to that recommended by Modak [11]. Figure 2 shows the radiative fraction, χ, as a function of the heat release rate [12] for this burner. The asymptotic behavior of constant χ can be seen at the higher flow rates. The curve designated HNG for "historic" natural gas will be used in subsequent calculations. This gas most closely resembles the gas used for the measurements in determining the gross features of these flames. Using natural gas for these systems Zukoski [13] finds χ to be about 25% based on a method of collecting the exhaust gases in a hood.

A crude check of figure 2 can be made by applying those results with the individual data (before scaling) of McCaffrey [2] where Q varied from 14 to 58 kW. The radiative components can be subtracted out of the total Q and the axial parameters in the plume region (the only regime where other data exist) can be determined and compared with literature values. The weighted averages of the centerline results become:

$$\frac{g\Delta T/T_o}{F_o^{2/3} z^{-5/3}} = 9.1 \tag{9}$$

$$\frac{V}{F_o^{1/3} z^{-1/3}} = 3.9 \tag{10}$$

where $F_o = \frac{g\,Q(1-\chi)}{\rho_o C_p T_o}$

This result is identical to Yokoi's [14] results for a point source system with negligible radiation.

Although from figure 2 the dependence of the radiative fraction upon total heat release appears significant, the square root dependence of χ in eq. (8) tends to diminish this effect on σ_v except for small fires. The asymptotic scaling, i.e., $\sigma_v \sim Q^{2/5}$ therefore can be used for calculating purposes provided it is not extrapolated to fires with ratios of flame height to fire base diameter small, i.e., $L/D \rightarrow 0$. Note the generality of eq. (8) for other fuels with very different radiative characteristics must yet be demonstrated. The $(1-\chi)^{1/2}$ in eq. *(8)* will be replaced by $(e-\chi)^{1/2}$ for systems with combustion efficiencies, e, signficantly less than 1. Using the asymptotic scaling.,

$$\frac{\sigma_v}{Q^{2/5}} = \alpha \frac{z}{Q^{2/5}} + \beta \tag{11}$$

will simplify the problem a great deal since Q will become a natural scaling parameter for m(z), H(z), etc. (see reference [1]) together with

$z/Q^{2/5}$ for scaled height. Note that a defined in (11) is $6\alpha_e/5$ where a_e is the normal entrainment coefficient from plume theory.

2.3 Non-Dissipative Plume

Substituting eq. (11) into eq. (8) will yield an expression containing three unknowns: a, β, and A - the three radial parameters for which the experimental results are in greatest disagreement. It is presumed that the centerline results A and B are known well enough from the measurements as is the radiative fraction, χ. Equation (8) states only that the value of $\frac{H}{Q}$ is $1 - \chi$ at the flame tip. It says nothing about the behavior in the plume region. .If radiation from the burnt gases in the plume is negligible compared with the radiation from the flame then H/Q will remain at the value determined at the flame tip. Radiative calculations based on estimated CO_2 and H_2O concentrations (and no soot) in the plume indeed substantiate this assumption. Since there are no other significant dissipative mechanisms in the plume, H/Q, for practical purposes, remains constant there and one can obtain an additional relation among the variables. That relation is $\frac{dH}{dz} = 0$ in the plume. For sooty flames zero will be replaced by a small negative number as will the combustion efficiency change as noted previously.

Taking the derivative of eq. (5) in the plume region and setting it equal to zero yields a relation for β/α in terms of A:

$$\frac{\beta}{\alpha} = z' \left| \frac{\kappa_\lambda + \lambda^2}{\kappa_\lambda/5 - \lambda^2} \right| \tag{12}$$

where

$$\kappa_A = (1 - \Gamma_\lambda)/[(\Delta T/T_o + 1)^{-1} - \Gamma_\lambda]$$

Note for the three Γ_λ functions (ignoring $\lambda = \infty$) in figure 1 it can be shown that

$$\frac{3}{5} z \frac{d\Gamma_\lambda}{dz} = \left(\Gamma_\lambda - \frac{1}{\Delta T/T_o + 1}\right) \cdot \lambda^2$$

Having now two expressions for the three unknowns, α and β can be solved for in terms of λ and compared with the experimental results of table I. Explicitly, α and β become:

$$\alpha = M\left(\frac{1}{5} - \frac{\lambda^2}{\kappa_\lambda}\right) \frac{L^{-5/6}}{\sqrt{1 - \Gamma_\lambda}} \tag{13}$$

$$\beta = M\left(1 + \frac{\lambda^2}{\kappa_\lambda}\right) \frac{L^{1/6}}{\sqrt{1 - \Gamma_\lambda}} \tag{14}$$

where

$$M = \frac{5}{6}\sqrt{\frac{1 - \chi}{\pi C_p \rho_o T_o A_p}}$$

and L is the flame length, $z' = 0.2\ \mathrm{m\ kW^{-2/5}}$.

3. Results

Figure 3 shows the result of plotting eqs. (13) and (14) as a function of λ. The data points are the results of the experiments. Also shown are results from the literature in non-combusting plumes. Note the literature results with $\beta = 0$ are for experiments with point heat sources or, the measurements were made so far from the source that the effect of the source size is lost. From figure 3 it would seem that the preponderance of evidence points to a $\lambda < 1$ contrary to the classical result of $\lambda = 1.16$.

Note the α/M portion of figure 3 could have been derived from point source plume theory results, eqs. (9) and (10). Letting $\sigma_v = \frac{6}{5} a_e z$ and

$$1 - \Gamma_\lambda = \frac{1}{1 + 1/\lambda^2}\left(\frac{\Delta T}{T_o}\right) - \frac{1}{1 + 2/\lambda^2}\left(\frac{\Delta T}{T_o}\right)^2 + \ldots$$

Substituting into eq. (6) yields, in the plume limit:

$$\frac{H}{Q} = \pi\left(\frac{6}{5}\right)^2 \frac{\tilde{A}\,\tilde{B}\,\alpha_e^2}{1 + 1/\lambda^2}$$

where $\tilde{A}$ and $\tilde{B}$ are the dimensionless, centerline experimental results in plume theory form (Eqs. (9) and (10)). Now, letting $\frac{H}{Q} \to 1$ the requisite relation between a and A is obtained. However, this analysis will yield no information about the all important intercept, β.

For the present measurements the slopes (a) appear to behave like the calculated result exceedingly well. The intercepts (β), on the other hand, are too wide by a factor of two! In fact, the calculated β hardly varies with A at all indicating that for a heat balance and a non-dissipative plume $\frac{\beta}{M} \sim .55(\mathrm{m \cdot kW^{-2/5}})^{1/6}$, a constant. The zero intercept or transverse extent at the burner surface appears to control the phenomena. If all the assumptions made in the above analysis are correct then both the cross correlation and pressure probe measurements are following some particular feature of the flame since the measured slopes follow the calculation. That feature is obviously not the l/e point of the velocity profile, since that would require the measured and analytical β to be the same. Perhaps the large scale eddy motion in the wings which is time averaged somehow tends to broaden the indicated profile. However, the distortion is conserved throughout the length of the flame since the slopes appear to be correct. Whatever the reason, figure 3 can be used as a framework for choosing reasonable radial parameters consistent with the experimental results. Before doing that it might be instructive to look at a graph of the actual data from table I.

Figure 4 shows the thermal profile, $\sigma_T/Q^{2/5}$ for both sets of flame and intermittent data plotted against height along with a least-squares fit. Within the scatter no significant difference exists between the two measurements which is not surprising since thermocouples, albeit of different sizes, were used for both data sets. Also shown on figure 4 are least squares fits to the velocity profile data (reference [2] data are presented in the form of eq. (11)). The differences in the two measuring techniques (and in λ seen in table I) are now clearly evident. The constraints of figure 3 as a function of λ can be sketched onto figure 4 for comparison. They are shown by crosses for the three λ of figure 1 at $z' = 0.2$. At $z' = 0$ one cross is shown since β is essentially constant, independent of λ. Note the constraints at the flame tip can be derived directly from the energy consideration alone, i.e., eq. (8) $\frac{H}{Q} \rightarrow 1 - \chi$. Wheieas, in order to obtain the constraints at the intercept, eq. (12), i.e., $\frac{dH}{dz} \rightarrow 0$ in the plume, must be incorporated into the analysis.

To continue the analysis it now becomes a matter of choosing a λ consistent with the measurements and eqs. (8) and (12). Since both measured a's seen on figure 3 appear to be consistent with the energy constraint (line) taking the mean of the measured λ seems reasonable. That will result in $\lambda = 0.77$ or $1/1.3$ which is very close to the recent measurements of Nakagome and Hirata [15] for a purely thermal plume. Note the difference between the mean and either measured A will produce a change in slope of the σ_V curves of figure 4 which is small compared with the shifts produced by the energy constraints reflected in B. That new position will be a line connecting the cross marks at $z' = 0$ and $z' = 0.2$. It can be assumed that the cross-correlation and pressure probe instrumentation systems are responding consistently but to different features of the large scale eddy motion in the wings of the flame. Note the time-averaged temperature results will be shifted a similar amount reflecting the same distortion seen by the other instruments.

Choosing $\lambda = 1/1.3$ will result in the following (from lines on figure 3) with $\chi = 0.26$:

$$\frac{\sigma_V}{Q^{2/5}} = 0.128 \frac{z}{Q^{2/5}} + 0.011 \quad \left[m \cdot kW^{-2/5}\right] \tag{11a}$$

Using the asymptotic scaling for σ_V eq. (4) becomes:

$$\frac{m(z)}{Q} = \pi \rho_o A \left(\frac{z}{Q^{2/5}}\right)^n \left(\alpha \frac{z}{Q^{2/5}} + \beta\right)^2 \Gamma_\lambda (\Delta T/T_o) \tag{4a}$$

where A and n and ΔT are the centerline average velocity and temperature rise results from table I and Γ_λ is determined from figure 1 at $\lambda = 1/1.3$.

Figure 5 is a plot of eq. (4a) for m/Q versus normalized height, $z/Q^{2/5}$. Also shown on the figure is H/Q calculated from eq. (6). At the flame tip $m/Q \simeq 0.007$ kg/s / kW which for CH_4 (50,000 kW / kg/s) corresponds to approximately 350 kg/s of air per kg/s of CH_4. Therefore the flame entrains approximately 20 times the stoichiometric air mass requirement (17.2) up to the end of the combustion region. This number is about 30% higher than the equivalence ratio of 0.067 ± 10% measured by Zukoski [13] using the hood collection technique (1/0.067 = 14.9). In order to fit his combustion plume model to a large quantity of flame height data Steward [16] found that only 400% excess air was entrained up to the flame tip. At the end of the continuous flame region, $z/Q^{2/5} = 0.08$ $m \cdot kW^{-2/5}$, the flame has entrained 90 times the methane flow or about 5 times the stoichiometric requirements. Mixing by the large-scale eddy motion would therefore appear to be the dominant controlling mechanism as opposed to any chemical effects. Note that

m/Q, H/Q as well as the scaled height, $z/Q^{2/5}$ are based on the total or net calorific potential heat release rate, Q, and not on H, the convective component.

H/Q rises rapidly to a value of approximately 0.4 at the flame-intermittent intersection and gradually rises to 0.74 at the intermittent-plume intersection. This number is simply 1 minus the radiative fraction which has been used to set the constants in the width function, σ_V.

Also plotted on figure 5 are the point source plume theory results of Yokoi [14] shown by the dashed lines. At the flame tip the mass flow rate predicted by plume theory is about 40% less than the present flame results. Also shown on figure 5 are measurements using a thistle-down tracer technique due to Thomas %&. [17] which agree quite well with the present results in the continuous flame region after which the shape deviates from both the present and plume results.

A good representation of eq. (4a) for calculating purposes in S.I. units is the following:

$$m/Q = 0.053\ (z/Q^{2/5})^{1.3} \tag{15}$$

valid up to the flame tip. It would be inappropriate to extend this result much beyond the flame tip since the radial data from table I are for the two lower regimes. In the plume region the point source results of Yokoi [14] ($m/Q = 0.063\ z'^{5/3}$) should begin to become valid, bearing in mind the turbulence contribution discussed in the Appendix. More recent analytical characterization [18] using momentum constraints in the lower regimes as well as the plume energy considerations discussed here leads to an expression for mass flow rate not very different from eq. (15) in the upper portion of the flame. Near the burner the results are somewhat different in that the mass flow rate and especially the heat flux rises more rapidly with height than do the present results.

A Note on Scaling:

Contrary to normal practice the variables plotted in the figures have, in general, not been made dimensionless. The reason for this is to emphasize the fact that no satisfactory scaling of buoyant diffusion flames has yet been realized. Note that $Q^{1/5}$ for velocity and $Q^{2/5}$ for length are <u>experimental</u> results. Froude model scaling, expected to be valid in the plume, utilizes the following scales, a function of burner or fire base diameter, D:

$$1 - D \qquad V \sim \sqrt{gD} \qquad Q \sim \rho_\Theta T_\Theta C_p \sqrt{gD}\ D^2 \qquad (\Delta T \sim T_o)$$

When the Froude number is "high" enough such that $L/D \sim (Q/D^{5/2})^{2/5}$ and χ = constant [12] one would expect this scaling to be valid (note for $D \sim Q^{2/5}$ Froude scaling would be consistent with the present measurements). However, for large enough fires ($L/D + 0$), those below the critical Froude No., flame heights and the radiative fraction become functions of <u>both</u> heat release rate and base diameter. Hasemi [19] has recently proposed a constant eddy diffusivity model utilizing the Boussinesq approximation in which the following scales, as a function of heat release rate, Q, were derived:

$$1 \sim \sqrt{C_p \rho K^3/g\beta Q} \qquad V \sim \sqrt{g\beta Q/C_p \rho K} \qquad \Delta T \sim Q/C_p \rho K$$

where K is the turbulent transfer coefficient, $\overline{U'V'} = -K\frac{au}{\partial x}$ and $\overline{U'T'} = -K\frac{\partial \Delta T}{\partial x}$. He shows that for $K = kQ^{3/5}$ where k is constant, the model will not only reproduce the experimentally determined scales 1/5 and 2/5, but also, will reproduce the detailed behavior of the intermittent regime extremely well. At the lower end of the intermittent regime near the continuous flame region where density differences become large the analysis, as expected, becomes weaker.

4. Summary and Conclusion

Expressions for mass and convective energy flux of buoyant diffusion flames from area sources have been obtained by an analysis using existing mean centerline velocity and temperature rise data from two different techniques. The method is based on a heat balance assuming negligible turbulent transport and a non-dissipative plume and utilizes an independent estimation of total radiative power output. Basically the width of the velocity profile is fixed by the balance of total heat release minus the radiative fraction at the flame tip together with the assumption of negligible radiative flux from the plume. On this basis the results indicate that both experimental techniques for measuring velocity overestimate the width of the fire plume by a considerable amount, possibly due to errors resulting from time averaging of the large-scale coherent structure in the wings. Horizontal or inflow velocity components cannot be discriminated against by either experimental technique and hence errors could result when the signal output is assumed to be simply the vertical component.

Although the present results are considerably higher than point source plume theory, further disagreements between measurements and plume theory calculations noted in the literature are possibly due to increased entrainment brought upon by disturbances to the free burn behavior, for example, by the door jet when the fire is located in an enclosure. Preliminary estimates of this effect are being pursued by Zukoski [13].

5. Acknowledgments

One of the authors (BJM) would like to thank the director and staff of the Fire Research Station for their assistance during his stay there as a guest worker.

6. References

[1] Cox, G.; Chitty, R. A study of the deterministic properties of unbounded fire plumes. Combustion and Flame. 39: 191; 1980.

[2] McCaffrey, B. J. Purely buoyant diffusion flames: some experimental results. Nat. Bur. Stand. (U.S.) NBSIR 79-1910; 1979 October.

[3] Ku, A.C.; Doria, M. L.; Lloyd, J. R. Numerical modeling of unsteady buoyant flows generated by a fire in a corridor; Sixteenth Symposium (Int.) on Combustion; The Combustion Institute; 1977. 1373.

[4] Emmons, H. W. The prediction of fires in buildings; Seventeenth Symposium (Int.) on Combustion; The Combustion Institute; 1978. 1101.

[5] Quintiere, J.; McCaffrey, B. J.; DenBraven, K. Experimental and theoretical analysis of quasi-steady small-scale enclosure fires; Seventeenth Symposium (Int.) on Combustion; The Combustion Institute; 1978. 1125.

[6] McCaffrey, B. J.; Rockett, J. A, Static pressure measurements of enclosure fires. J. Res. Nat. Bur. Stand. (U.S.). 81: 107; 1977.

[7] Rouse, H.; Yih, C. S.; Humphreys, H. W. Gravitational convection from a boundary source. Tellus. 4: 201; 1952.

[8] Terai, T.; Nitta, K. Experiments on plume rising from burning heat source with finite sizes. Proc. Symp. Arch. Inst.; Japan; 1976.

[9] Markstein, G. H. Scaling of radiative characteristics of turbulent diffusion flames; Sixteenth Symposium (Int.) on Combustion; The Combustion Institute; 1976. 1407.

[10] Modak, A. T.; Croce, P. A. Plastic pool fires. Combustion and Flame. 30: 251; 1977.

[11] Modak, A. T. Thermal radiation from pool fires. Factory Mutual Research; Norwood, Massachusetts. TR 22361-5; 1976 August.

[12] McCaffrey, B. J. Measurements of the radiative power output of some buoyant diffusion flames. Western States Section Combustion Institute Paper No. WSS/CI 81-15.

[13] Zukoski, E. E.; Kubota, T.; Cetegen, B. Entrainment in fire plumes. Fire Safety Journal. 3: 107; 1981.

[14] Yokoi, S. Study on the prevention of fire-spread caused by hot upward current. Report of the Building Research Institute; Ministry of Construction; Japan; No. *34;* 1960 November.

[15] Nakagome, H.; Hirata, M. The structure of turbulent diffusion in an axi-symmetrical thermal plume, in heat transfer and turbulent buoyant convection. Spalding, D. B.; Afgan, N.; eds. Washington, D. C.: Hemisphere Publishing Corporation; 1977. 361.

[16] Steward, F. R. Prediction of the height of turbulent diffusion buoyant flames. Combustion Science and Technology. 2: 203; 1970.

[17] Thomas, P. H.; Baldwin, R.; Heselden, A. J. M. Buoyant diffusion flames: some measurements of air entrainment, heat transfer, and flame merging; Tenth Symposium (Int.) on Combustion; The Combustion Institute; 1965. **983-996.**

[18] McCaffrey, B. J. Momentum implications for buoyant diffusion flames; abstract presented at Eastern States Section Meeting; The Combustion Institute; Pittsburgh; 1981.

[19] Hasemi, Y. Properties of the intermittent flaming region in the upward current above a diffusion flame; Proc. Ann. Meeting JAFSE; 1981. 13.

[20] Kotsovinos, N. E.; List, E. J. Plane turbulent buoyant jets. Journal of Fluid Mechanics. 81: 25; 1977.

[21] George, W. K.; Alpert, R. L.; Tamanini, F. Turbulence measurements in an axi-symmetric buoyant plume. Int. J. of Heat and Mass Transfer. 20: 1145; 1977.

[22] Cox, G.; Chitty, R. Unpublished data; 1980.

Appendix A. Turbulent Transport

It is instructive to examine the assumption that the turbulent transport of heat and mass can be ignored. If pressure fluctuations are assumed to be small then it is possible to show that

$$m(z) = \int_0^\infty \bar{\rho}_m \cdot \bar{v} \left\{ 1 + \gamma^2\left(\frac{\overline{T'^2}}{\overline{\Delta T}^2}\right) - \gamma\left(\frac{\overline{V'T'}}{\overline{V}\cdot\overline{\Delta T}}\right) + \gamma^2\left(\frac{\overline{V'T'^2}}{\overline{V}\cdot\overline{\Delta T}^2}\right)\right\} 2\pi x dx \tag{A-1}$$

and

$$H(z) = \int_0^\infty \bar{\rho}_m \cdot \bar{V} \cdot \overline{\Delta T} \left\{ 1 - \left(\frac{1}{\gamma} - 1\right)\gamma^2\left(\frac{\overline{T'^2}}{\overline{\Delta T}^2}\right) \right.$$

$$\left. + \left(\frac{1}{\gamma} - 1\right)\gamma\left(\frac{\overline{V'T'}}{\overline{V}\cdot\overline{\Delta T}}\right) - \left(\frac{1}{\gamma} - 1\right)\gamma^2\left(\frac{\overline{V'T'^2}}{\overline{V}\cdot\overline{\Delta T}^2}\right)\right\} C_p 2\pi x dx \tag{A-2}$$

where the usual Reynolds decomposition of V, p and AT have been used.

$$\gamma = \frac{1}{1 + \frac{T_o}{AT}}$$

$$\bar{\rho}_m = \frac{\rho_o T_o}{\overline{\Delta T} + T_o}$$ is the density based on the mean temperature

not the true mean density which is $\bar{\rho} = \frac{\rho_o T_o - \overline{\rho' T'}}{\overline{AT} + T_o}$

Only the first term in eq. (A–2) has been used to assess total heat flux. Inspection of the "extra terms" in these expressions shows that both over and underestimates are possible if the first term alone is used.

For small AT ($y \div 0$) the $V'T'$ term dominates leading to an underestimate of total heat flux. The data of Kotsovinos and List [20] and of George ~~et al~~. [21] support this conclusion. George estimates that 85% of the vertical heat transport is carried by the mean flow. However, for different temperature levels more complex phenomena may be taking place. For example, for AT = T_o (say), at the flame tip and assuming the triple correlation is small:

$$H(z) = \int_0^\infty C_p \bar{\rho}_m \cdot \bar{V} \cdot \overline{\Delta T} \left\{ 1 - \frac{1}{4}\left(\frac{\overline{T'^2}}{\overline{\Delta T}^2}\right) + \frac{1}{2}\left(\frac{\overline{V'T'}}{\bar{V}\cdot\overline{\Delta T}}\right) \right\} 2\pi x dx \qquad \text{(A-3)}$$

In a conventional plume George et al. [21] measured peak values of $(T'^2)^{1/2}/\overline{AT}$ at 0.4 and $\overline{V'T'}/\bar{V}\cdot\overline{\Delta T}$ at 0.07. The transverse distribution of these parameters was wider than for V and AT so that "top-hat" profiles could be assumed. Although no measurements of V'T' have been made in fire plumes, recent measurements of $(T'^2)^{1/2}/\overline{\Delta T}$ [22] indicate maxima at the flame tip of between 0.4 to 0.7. Overestimates of total flux might then be expected if $\overline{V'T'}/\bar{V}\cdot\overline{\Delta T}$ is less than between .08 to .25. So both underestimates and overestimates based on mean flux are possible in different regions of the flame system making the need for time resolved measurements critical.

For the present any underestimate or overestimate of Q will be reflected in M, i.e, $1 - \chi$ should be increased or decreased. Hence a and β will vary by the square root of the change but $m(z)$ and $H(z)$ are functions of α and β to the second power. The change will therefore be directly reflected in m and H. If for example the lack of accounting for turbulence leads to a 15% overestimate of H then in figure 5 below the flame tip H should be reduced by 15%. If George's [21] contention is correct then somewhere above the flame tip the curves would have to be increased by 15%. Assuming there is a smooth transition between this decreasing and increasing of the mean result, the mean result will overestimate in the flame region, pass through the 'correct value' and then begin to underestimate in the plume region and therefore on a height-averaged basis yield something close to valid results.

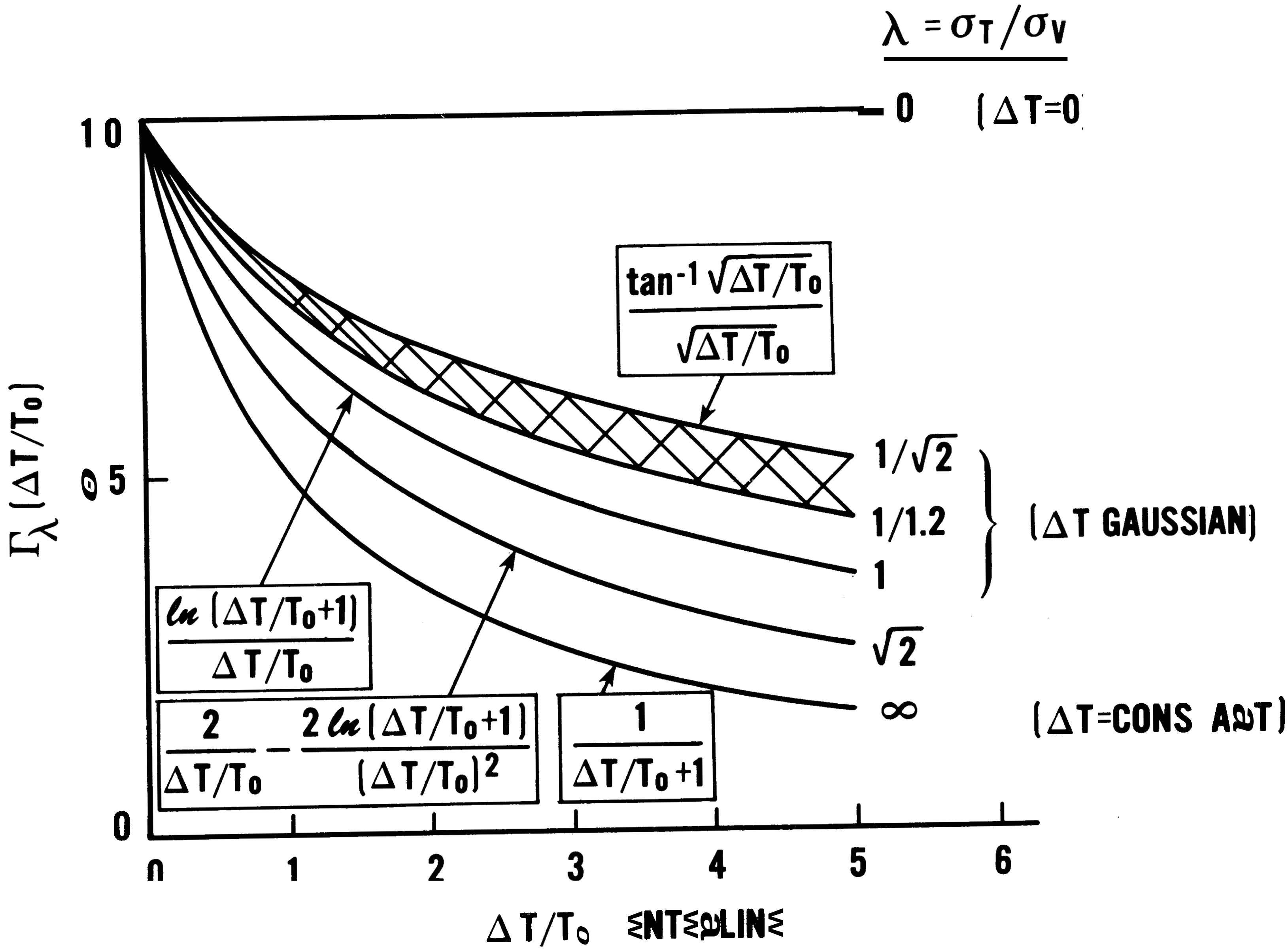

Figure 1. $\Gamma_\lambda(\Delta T/T_0)$ plotted against $\Delta T/T_0$ for various λ

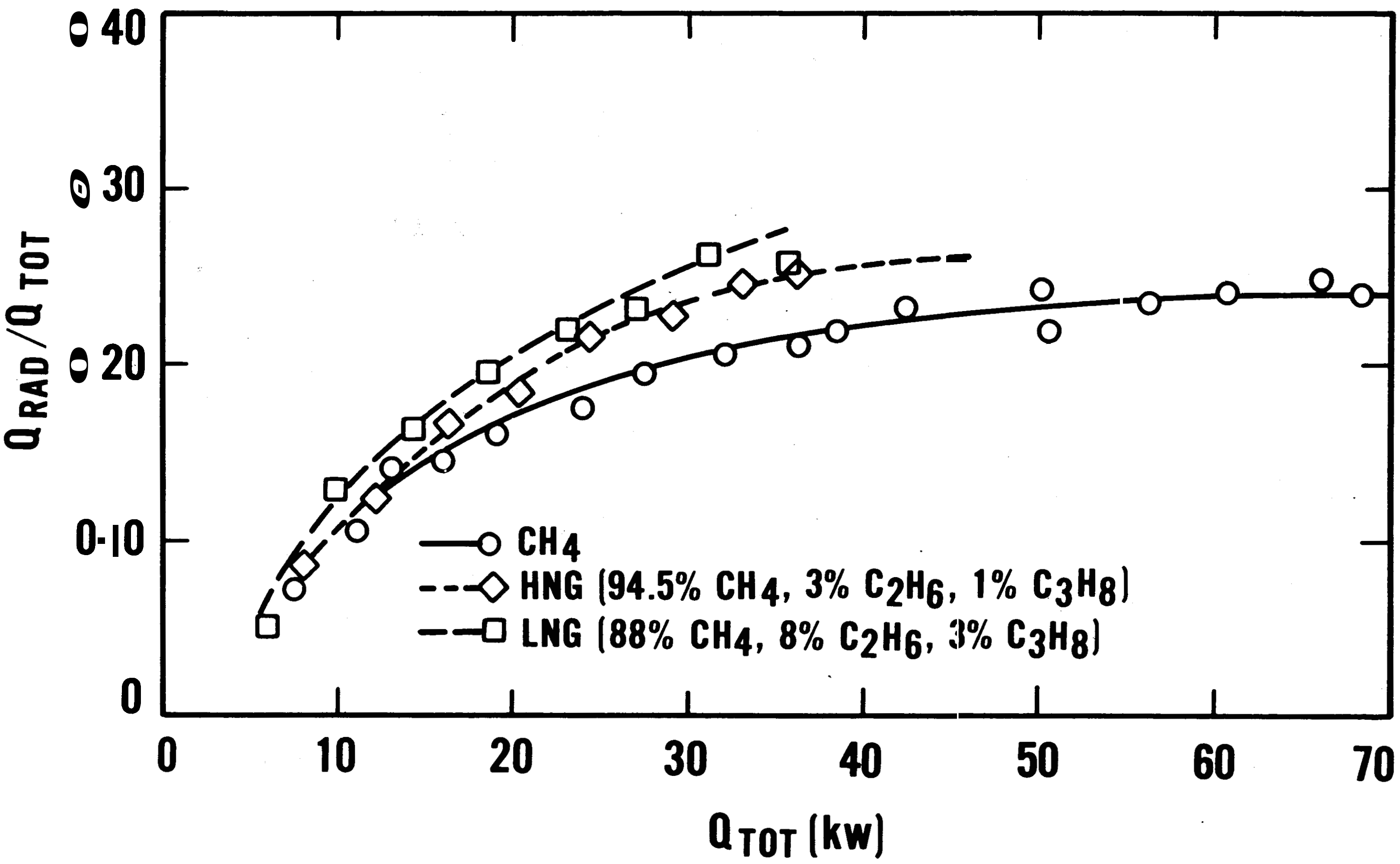

Figure 2. The radiative fraction, χ, as a function of the total heat release rate

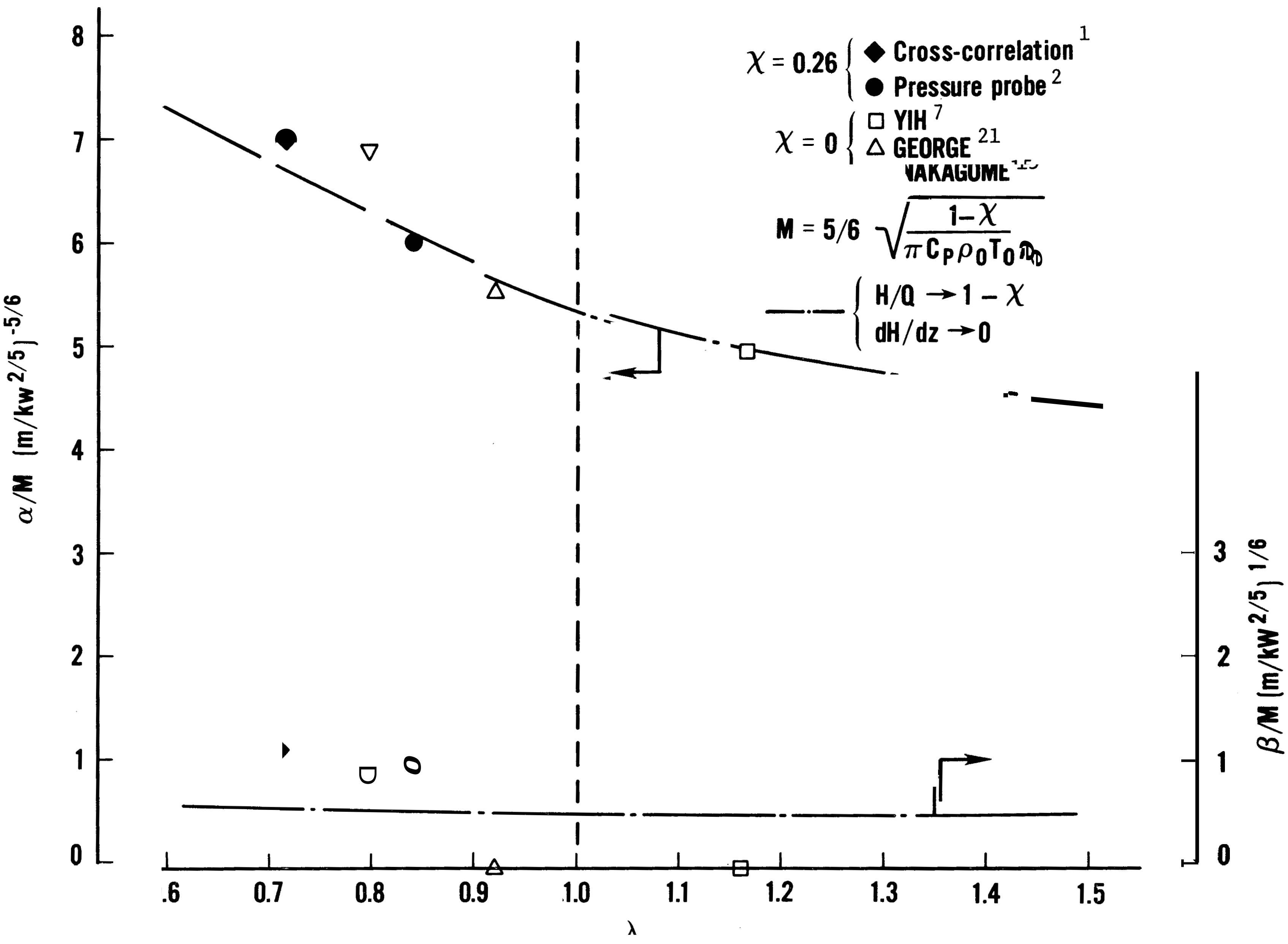

Figure 3. The radial parameters (α, β) as a function of λ

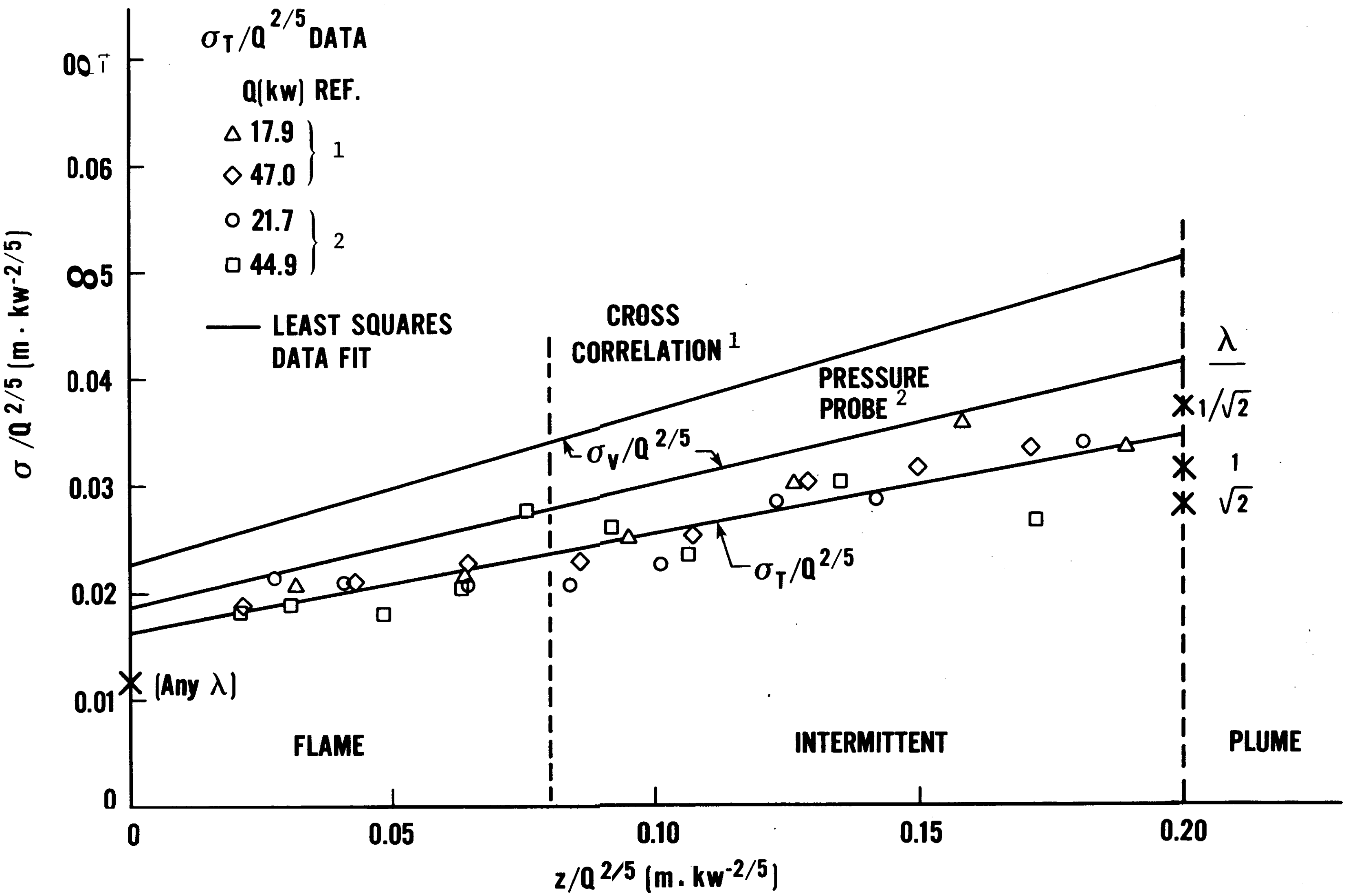

Figure 4. Temperature and velocity profile data at various distances above the burner

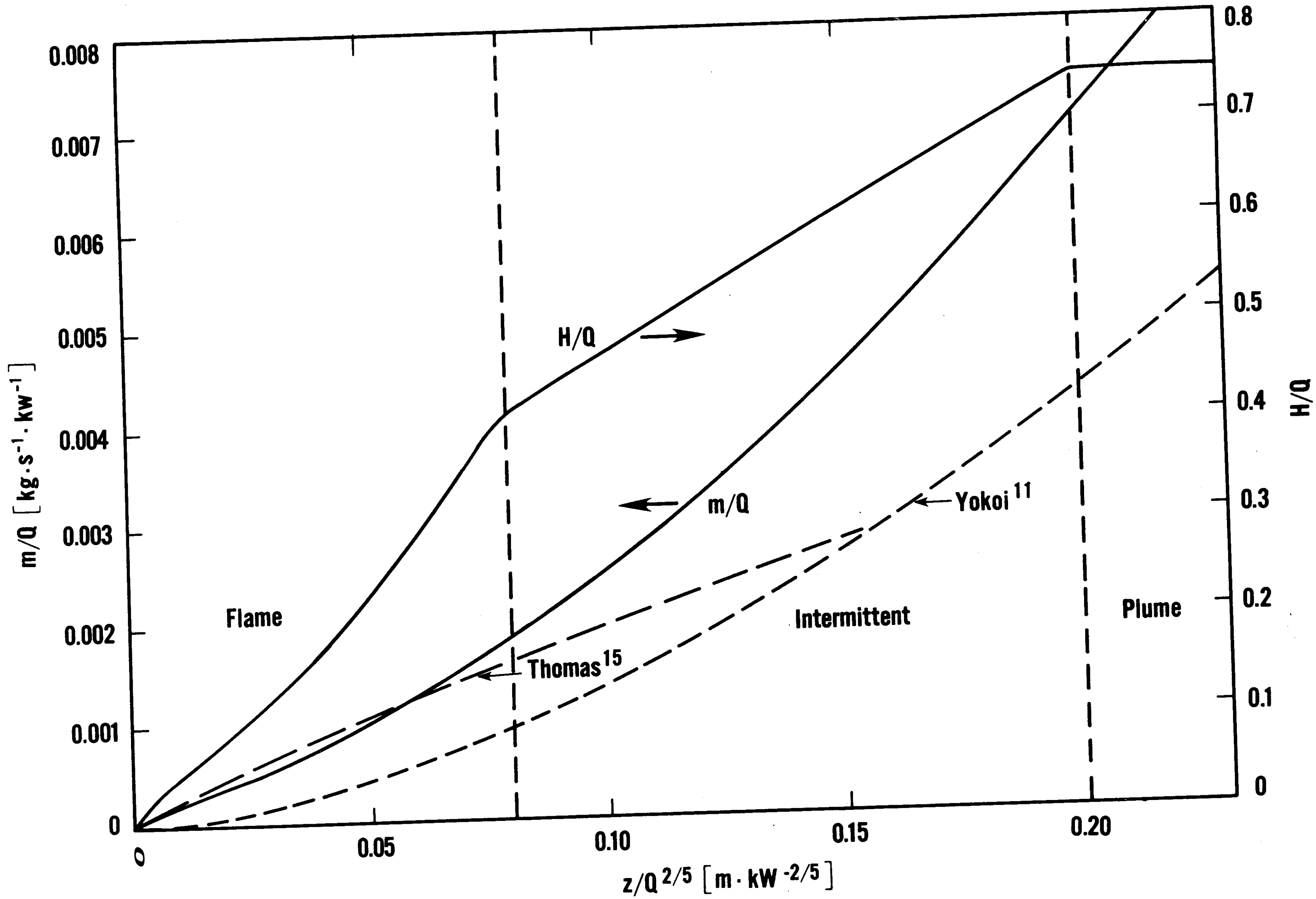

Figure 5. Calculated mass and energy fluxes as a function of height

U.S. DEPT. OF COMM. BIBLIOGRAPHIC DATA SHEET *(See instructions)*	1. PUBLICATION OR REPORT NO. NBSIR 82-2473	2. Performing Organ. Report No.	3. Publication Date February 1982

4. TITLE AND SUBTITLE

Entrainment and Heat Flux of Buoyant Diffusion Flames

5. AUTHOR(S)

B. J. McCaffrey and G. Cox

6. PERFORMING ORGANIZATION *(If joint or other than NBS, see instructions)*

NATIONAL BUREAU OF STANDARDS
DEPARTMENT OF COMMERCE
WASHINGTON, D.C. 20234

7. Contract/Grant No.

8. Type of Report & Period Covered

Final

9. SPONSORING ORGANIZATION NAME AND COMPLETE ADDRESS *(Street, City, State, ZIP)*

10. SUPPLEMENTARY NOTES

☐ Document describes a computer program; SF-185, FIPS Software Summary, is attached.

11. ABSTRACT (A *200-word or less factual summary of most significant information. If document includes a significant bibliography or literature survey, mention it here)*

Measurements of the vertical component of velocity in buoyant diffusion flames from extended sources by both cross-correlation and pressure probe techniques incorporating time-average signal processing appear to overestimate the transverse size of these systems based on a heat balance using measured mean flux. By utilizing measurements of the radiative fraction of the flames, and forcing a mean flux heat balance, estimates of the transverse variation of velocity are obtained and expressions for flame entrainment and convective heat flux are determined. The use of mean values is seen to lead to both overestimates as well as underestimates of total flux due to turbulent transport.

12. **KEY WORDS** *(Six to twelve entries; alphabetical order; capitalize only proper names; and separate key words by semicolons)*

Buoyancy; cross-correlation; diffusion flames; entrainment; heat flux; radiation; turbulence

13. AVAILABILITY

- [XX] Unlimited
- ☐ For Official Distribution. Do Not Release to NTIS
- ☐ Order From Superintendent of Documents, U.S. Government Printing Office, Washington, D.C. 20402.
- [XX] Order From National Technical Information Service (NTIS), Springfield, VA. 22161

14. NO. OF PRINTED PAGES

35

15. Price

$7.50